RSC Advances

ROYAL SOCIETY OF CHEMISTRY

www.rsc.org/advances

Journal Name

ARTICLE

A novel self-activated white-light-emitting phosphor of Na_2TiSiO_5 with two Ti sites of TiO_5 and TiO_6

Received 00th January 20xx,
Accepted 00th January 20xx

DOI: 10.1039/x0xx00000x

www.rsc.org/

Jianyan Ding, Yanyan Li, Quansheng Wu, Qiang Long, Yichao Wang and Yuhua Wang*

In this work, a novel self-activated light emitting phosphor of Na_2TiSiO_5 (NTSO) has been successfully synthesized by high temperature solid-state reaction. The photoluminescence (PL) and cathodoluminescence (CL) properties of the NTSO have been measured. Under the excitation at 260 nm, NTSO emits a white light with the CIE chromaticity coordinates (0.275, 0.355) and the cyan light can also be observed at low voltage excitation. The crystal structure of NTSO has been investigated using the Rietveld refinement, which shows that Ti ions not only occupy the octahedron center but also connect with five O ions to form TiO_5 polyhedron. The special polyhedron of TiO_5 broadens the emission band, and the energy transfer between the two sites has also been proved through the time-resolved photoluminescence (TRPL) spectra. Finally, CL properties of NTSO with a function of the accelerating voltage, filament current and electron radiation time have been measured and the results show that NTSO has bright light, excellent stability and good CIE chromaticity coordinates, which indicates that NTSO have the potential to be applied in FEDs.

1. Introduction

In recent years, rare-earths activated phosphors have received considerable attention because they not only can combine with blue InGaN LED chip to form the white light emitting diodes (WLEDs), but also play a important role in Field-emission displays (FEDs). As we know, WLEDs have many excellent advantages, such as: high brightness, low energy consumption and environment friendly,[1-4] and FEDs can provide a display with a thin panel, wide viewing, quick response time, high contrast ratio, light weight, and low power consumption.[5-6] In another word, rare-earths activated phosphors occupy the main part in the field of lighting and displays. However, the recent limited supply and the increased demand for rare-earth elements have restricted their application. Therefore, it is necessary to find novel activators acting as luminescent centers to replace the rare-earth.

The same as rare-earth, the bright light can also be obtained by the transition metal resulted by the d-d transition like Mn, Cr ions. Recently, Ti activated phosphors have gradually been explored and reported such as: $A_2Sn_{1-x}Ti_xO_4$ (where A = Mg, Ca, Sr, Ba, and Zn),[7-13] $BaM_{1-x}Ti_xSi_3O_9$ (where M = Sn and Zr),[14,15] $Mg_5Sn_{1-x}Ti_xB_2O_{10}$,[16] $Mg_3Zr_{1-x}Ti_xB_2O_8$,[16] $AZr_{1-x}Ti_x(BO_3)_2$ (A = Ca, Sr, and Ba),[17] $CaSn_{1-x}Ti_x(BO_3)_2$,[18] $CaSn_{1-x}Ti_xSiO_5$,[19] and $Ca_3Sn_{1-x}Ti_xSi_2O_9$.[19]. And it can be observed that Ti^{4+} ions commonly replace the Sn^{4+} or Zr^{4+} ions to build up TiO_6 octahedrons, which emit a blue light with the emission band ranging from 430 nm to 480 nm. However, in this work, Ti^{4+} ions not only enter into the center of the octahedrons but also make up the TiO_5 polyhedrons, and this finally broadens its emission band.

A phase diagram of the Na_2O-TiO_2-SiO_2 system has been provided by Glasser and Marr[20]. The natural occurrence of natisite, given as Na-Ti orthosilicate ($Na_2TiOSiO_4$), has only been reported by Bussen et al.[21] in 1975 as being a post-magmatic hydrothermal product associated with an alkalic granitoid massif in the Kola Peninsula, Russia. It has been shown to give a bright blue luminescence by X-ray irradiation.[22] However, the PL and CL properties of the NTSO have never been reported. In this work, a white light and the cyan light with the peak at around 500 nm can be detected under the excitation at 260 nm and low voltage excitation, respectively. The luminescent properties resulted from the two sites of Ti ions have been analyzed in detail, and the energy transfer between the TiO_5 and TiO_6 has also been proved by the TRPL spectra. Finally, various accelerating voltage, filament current and electron radiation time have been measured to indicate its potential application in the FEDs.

2. Experiment section

2.1 Material and synthesis

The phosphor of NTSO has been synthesized by a high temperature solid-state reaction. The raw materials used for the

Key Laboratory for Special Function Materials and Structural Design of the Ministry of the Education, School of Physical Science and Technology, Lanzhou University, Lanzhou, 730000, China. E-mail: wyh@lzu.edu.cn; Fax: +86-931-8913554; Tel: +86-931-8912772.

prepared phosphor were NaOH (A.R., >99.50%), TiO_2 (A.R., >99.90%), SiO_2 (A.R., >99.999%). Stoichiometric amounts of reactants were mixed and ground in an agate mortar, and then the final mixture was placed in to an Al_2O_3 crucible. Finally, the mixture was annealed at 850 ℃ for 4 h. After that, the samples were furnace-cooled to room temperature, and ground again into powders for measurements.

2.2 Measurement and characterization

The photoluminescence (PL) and photoluminescence excitation (PLE) were measured by a FLS-920T fluorescence spectrophotometer equipped with a 450W Xe light source and double excitation monochromators. Diffuse reflectance ultraviolet-visible (UV-vis) absorption spectra were measured using a Perkin Elmer 950 spectrometer. The crystal structures of the synthesized samples were identified by X-ray powder diffraction (XRD) using a Rigaku D/max–2400 X diffraction with Ni-filtered Cu Kα radiation. All of the measurements were performed at room temperature. Thermal quenching was tested using a heating apparatus (TAP-02) in combination with PL equipment. The morphology of the powder was investigated by scanning electron microscopy (SEM, S-340, Hitachi, Japan).

3. Results and discussion

3.1 Crystal structure and phase identification

In order to investigate the crystal structure of NTSO, especially for the coordination environments of the Ti^{4+} ions, the Retiveld structural refinements for NTSO were studied based on the general structure analysis system (GASA) program[23] and the calculated, observed and different results for the Retiveld refinement XRD patterns are shown in Fig. 1(a). All of the observed peaks satisfy the reflection condition and converge to R_{wp} = 9.4 %, R_p = 7.9 % and χ^2 = 1.726. As exhibited in Fig. 1(b), NTSO crystallizes in an orthorhombic crystal system with space group Pmc 21(26) and lattice parameters of a = 9.1222(5) Å, b = 4.8040(3) Å, c = 9.8293(5) Å, respectively. The detail crystal data of NTSO have been shown in Table 1. There are two cation sites for Ti ions to occupy. One cation site connect with five O ions, another is located at the distorted octahedron center with Oh point group system, which connects with six O atoms. The bond lengths of Ti-O have been exhibited in Fig. 1(c), and the average bond lengths of TiO_5 and TiO_6 are calculated as 1.8833 Å and 2.1062 Å, respectively. The shorter bond length of TiO_5 exhibits a stronger crystal field strength compared with TiO_6, and this crystal field strength is expected to change the emission spectrum. The two kinds of Ti polyhedrons connect with each other through SiO_4 tetrahedron, and the eight-membered ring made up by the Ti polyhedron and Si tetrahedron is shown in Fig. 1(d), which forms the main framework of the NTSO through the corner-shared way. And Na^+ ions occupy octahedral interstitial position to realize the charge balance.

Table 1 The crystal data of NTSO from the Retiveld refinement

Formula	Na_2TiSiO_5		
Crystal system	orthorhombic		
Space group	Pmc 21(26)		
Cell parameters	a = 9.1222(5) Å, b = 4.8040(3) Å, c = 9.8293(5) Å.		
Cell volume	430.75(4) $Å^3$		
Z	4		
Atom	X/a	Y/b	Z/c
Ti1	1/2	0.46766	0.00603
Ti2	0	0.02073	0.77895
Na1	1/2	-0.00164	0.25105
Na2	0.24828	0.00449	0.01486
Na3	0	0.41036	0.498232
Si1	0.25568	0.51049	0.25147
O1	1/2	0.80371	-0.00516
O2	0.35190	0.35960	0.13340
O3	0.35430	0.64520	0.36430
O4	0	0.86815	0.43466
O5	0.14639	0.75258	0.18840
O6	0.14212	0.27468	0.31707

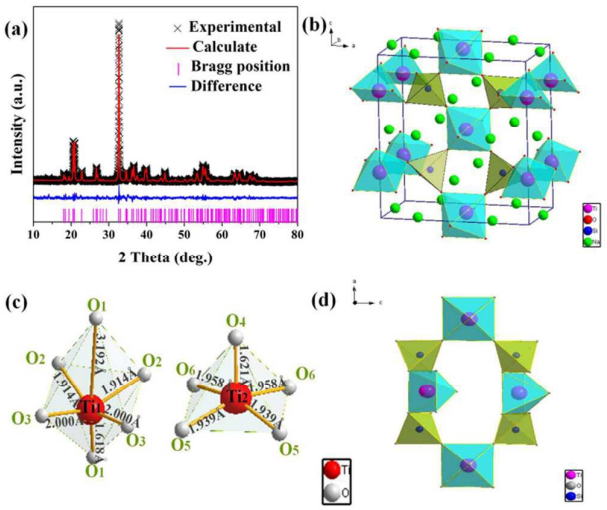

Fig. 1 (a) The experimental (crosses) and calculated (red solid line) XRD profiles and their different (blue line) for the Retiveld refinement of NTSO. (b) The crystal structure of NTSO. (c) The coordination environment of the three Ti^{4+} sites with the bond lengths of Ti^{4+}-O^{2-}. (d) The eight-membered ring made up by the Ti polyhedron and Si tetrahedron.

The morphology of NTSO is shown in Fig. 2. The irregular morphology of NTSO has been observed and the sample shows a good dispersion. The particle size distribution of NTSO has also been investigated by the program of Nano Measurer. The results indicate that the particle size of NTSO ranges from 0.5 μm to 5 μm and the average diameter of NTSO is 1.60 μm.

3.2 Luminescent properties.

Fig. 3(a) shows the diffuse reflection and adsorption spectra of NTSO, and the excitation spectrum monitored at 500 nm has also been exhibited for comparison. The NTSO has a strong absorption ranging from the 400 nm to 200 nm. It is obviously observed that two peaks located at around 290 nm and 390 nm can be separated, which is consistent with the excitation

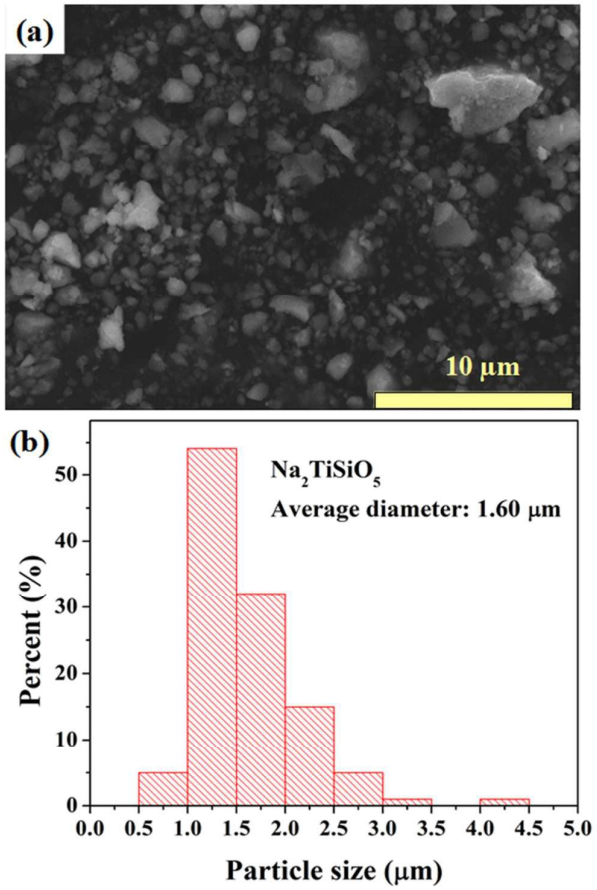

Fig. 2 SEM micrograph of NTSO (a). The particle size distribution of NTSO (b).

spectrum of NTSO. According to the Retiveld structural refinements for NTSO, we have drawn the energy-level diagram of TiO_6, which is shown in Fig. 3(b). As we know, the 3d level is the outmost electron orbital of the Ti^{4+} ions, which are not shielded completely by the outer environment. Therefore, the split levels are determined by the symmetry around Ti^{4+} ions. The 3d level of Ti^{4+} ions contains five electron orbitals, and they are d_{xy}, d_{xz}, d_{yz},d_{x2-y2} and d_{z2}, respectively. When Ti^{4+} ions occupy the site with Oh symmetry, the 3d orbitals of Ti^{4+} ions will split into two levels, which are T_2 and E_g, respectively. The T_2 level contains three orbitals (d_{xy}, d_{xz} and d_{yz}) and the other orbitals (d_{x2-y2} and d_{z2}) belong to E_g energy level. The E_g level and the 2p orbitals of O^{2-} ions would build up a bonding orbital and an antibonding orbital. In this model, Ti^{4+} ions have a tendency to be reduced to Ti^{3+}. Therefore, the electrons would transfer from the ground state to the antibonding orbital, which is the charge transfer band of O^{2-}-Ti^{4+}. Meanwhile, the T_2-E_g transition of electrons can also be observed and it has a little contribution for the light emitting, which is corresponding to the excitation spectrum. According to the above discussion, the two absorption peaks located at 290 nm and 390 nm can be attributed to the charge transfer band of O^{2-}-Ti^{4+} and the T_2-E_g transition of electrons, respectively.

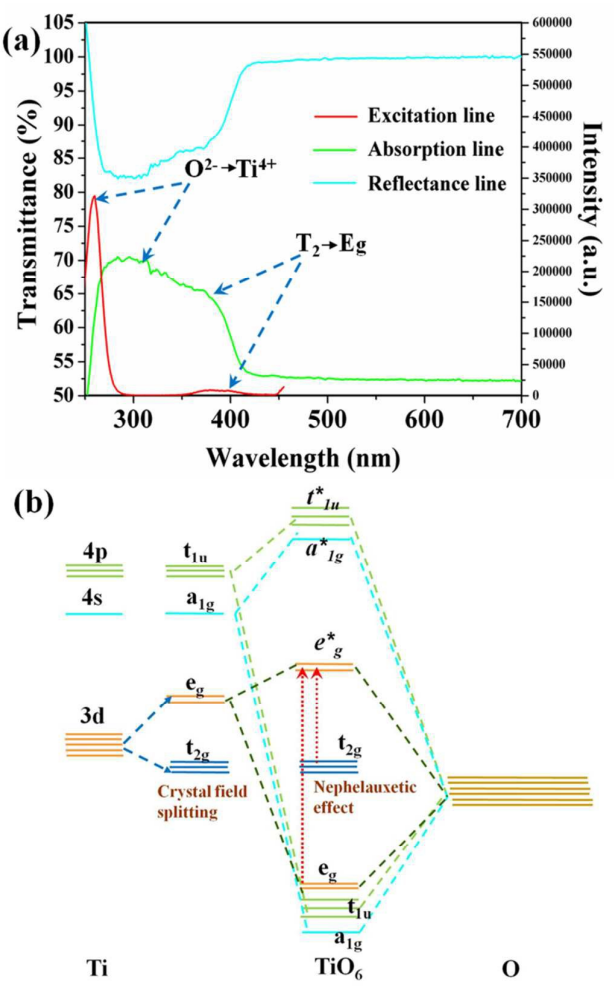

Fig. 3 (a) The reflectance, absorption and PLE spectra of NTSO. (b) The energy level diagram of NTSO.

Fig. 4(a) exhibits the emission spectrum of the NTSO. Under the excitation at 260 nm, the NTSO emits a white light with a broad emission band ranging from 400 nm to 650 nm. The emission band can be deconvoluted into four well-separated Gaussian components with the peaks at 450 nm (2.7555 eV), 490 nm (2.5306 eV), 555 nm (2.2342 eV) and 625 (1.9840 eV) nm. As the calculated energy, it can be found that the energies of E_1 (2.5306 eV (490 nm)+2.2342 eV (555 nm) = 4.7642 eV) and E_2 (2.7555 eV (450 nm)+1.9840 eV (620 nm) = 4.7395 eV) are close to the energy of the excitation spectrum peaked at 260 nm (4.7692 eV). Therefore, we deduce that the emission peaks located at 490 nm and 555 nm and the peaks located at 450 nm and 625 nm belong to different sites of Ti ions. Considering the coordinate environment of Ti^{4+}, the energy separation between the T_{2g} and E_g energy level 10Dq can be calculated by the following equation:[24]

$$10\,Dq = 5Ze2(r^4)/12a \quad (1)$$

where Ze is the charge on the ligand ion, (r^4) is the average value of r^4 for 3d orbital and a is the average distance between the central ion and ligand oxygen ions. Compared with the bond length, the crystal field splitting of TiO_5 is stronger than

TiO_6, which leads to the red-shift of the emission band. Therefore, it is reasonably deduced that emission peaks located at 490 nm and 555 nm belong to TiO_5 and the other peaks belong to TiO_6 (450 nm and 625 nm). The same blue light has also been found in $CaZr_{1-x}Ti_xO_3$ (431 nm emission)[25] $Ca_2Sn_{1-x}Ti_xO_4$ (445 nm emission) [11] $Mg_5Sn_{1-x}Ti_xB_2O_{10}$ (430 nm emission)[17] and $BaZr_{1-x}Ti_xSi_3O_9$ (450 nm emission)[14], which exhibit that Ti^{4+} connect with six O^{2-} ions to form the TiO_6 octahedron with average bond lengths ranging from 2.013 to 2.417 Å. And the shorter average bond length of TiO_5 (1.8833 Å) shows a stronger crystal field strength, which leads to the emission peak changing from blue to blue-green.

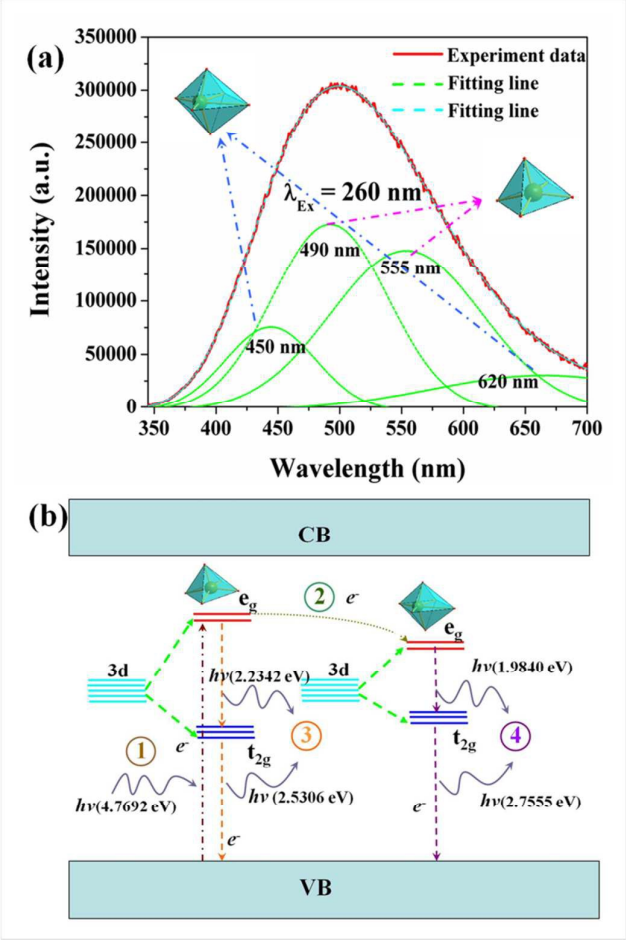

Fig. 4 (a) The PL spectrum of NTSO. (b) The energy level diagram of Ti ions occupying two sites.

Fig. 4(b) shows the energy diagrams of Ti^{4+} in the different sites. According to the above calculation, it can be seen that the electron absorbing the activated energy (4.7692 eV) can transfer from the ground state to the E_g energy level along the way ① and partial electrons would transfer to another site along the way ②. Then the electrons would return to the ground state along the way ③ and ④ to emit visible light. In this process, electrons would have a relaxation, which is the reason why the

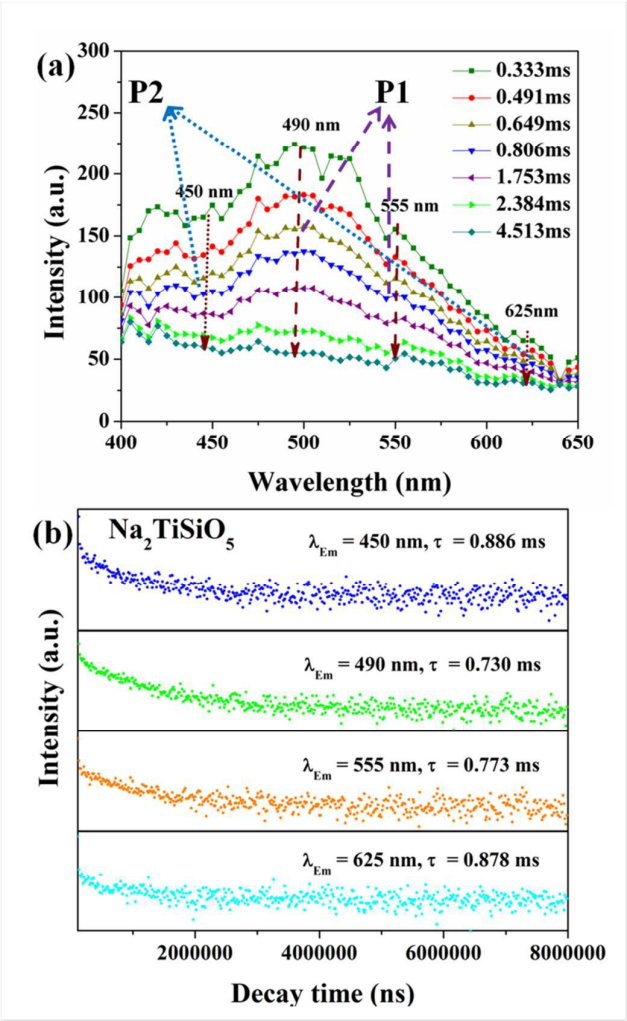

Fig. 5 (a) The TRPL spectra of NTSO. (b) The lifetime Decay curves of NTSO monitored at different emission peaks.

energy E_1 (4.7642 eV) and E_2 (4.7395 eV) is smaller than the excitation energy (4.7692 eV).

In order the further investigate the relationship between the two Ti sites and their contribution to the luminescence properties of NTSO, a series of lifetime decays of NTSO were measured at different wavelengths from 400 nm to 650 nm at 5 nm intervals. The time-resolved photoluminescence (TRPL) spectra and the lifetime decay curves of NTSO have been shown in Fig. 5(a) and (b). In this regard, it is clear that P1 comes from the Ti1 site peaking at 490 nm and 555 nm and P2 comes from the Ti2 site peaking at 450 nm and 625 nm. With the increase of the decay time, the trends of the time evolution of P1 and P2 are the same. However, it is obvious that the time revolution of the P1 component was much faster than that of the P2 component, which leads to the Ratio of P1/P2 decreasing drastically from 1.27 to 0.57 with the increase of the decay time. According to the TRPL results, the energy transfer from the TiO_5 to TiO_6 would take place in the host lattice of NTSO, which is corresponding to the above deduction.

It can be seen that the curves can be well fitted by a second-order exponential decay curve using the following biexponential equation:[26-28]

$$I = A_1\exp(-t/\tau_1) + A_2 \exp(-t/\tau_2) \quad (2)$$

where I is the luminescence intensity; t is the time; A_1 and A_2 are fitting constants, τ_1 and τ_2 are short and long lifetimes for exponential components, respectively. Therefore, the average lifetime τ can be obtained by the formula as follows:[29-31]

$$\tau = (A_1\tau_1^2+A_2\tau_2^2)/(A_1\tau_1+A_2\tau_2) \quad (3)$$

On the basis of the above formula, the average lifetimes τ of NTSO peaked at 445 nm, 490 nm, 555 nm and 620 nm are 0.785, 0.730, 0.773 and 0.878, respectively.

Fig. 6 (a) shows the CL emission spectrum of NTSO with two obvious emission peaks located at 450 nm and 490 nm, and the result is different from PL properties, which indicates that the emission light of NTSO is dependent on the excitation sources. The CL properties of NTSO as the function of the accelerating voltage and the filament current have also been investigated and exhibited in Fig.6 (b) and (d), respectively. When the filament current is fixed at 50 mA, the CL intensity increases as the raising of the accelerating voltage from 1 kV to 6 kV. Similarly, as the increase of the filament current from 30 mA to 90 mA, the CL intensity shows an obvious increase with the accelerating voltage fixed at 5 kV. This phenomenon is due to the deeper penetration of the electrons into the phosphor body and the larger electron beam current density. The electron penetration depth can be estimated using the empirical formula:[32] $L = 250(A/\rho)(E/Z^{1/2})^n$, where $n = 1.2/(1-0.29\lg Z)$, ρ is the bulk density, Z is the atomic number or the number of electrons per molecule in the case compounds, A is the atomic or molecular weight of the material and E is the accelerating voltage. For NTSO, $\rho = 3.11402$ g/cm^3, A = 201.9290 and Z = 36, the estimated electron penetration depth at 1.5 kV is about 3.1269 nm. For CL, the Ti^{4+} ions are excited by the plasma produced by the incident electrons. The deeper the electron penetration depth, the more plasma will be produced, which results in more Ti^{4+} ions being excited and thus, the CL intensity increases.

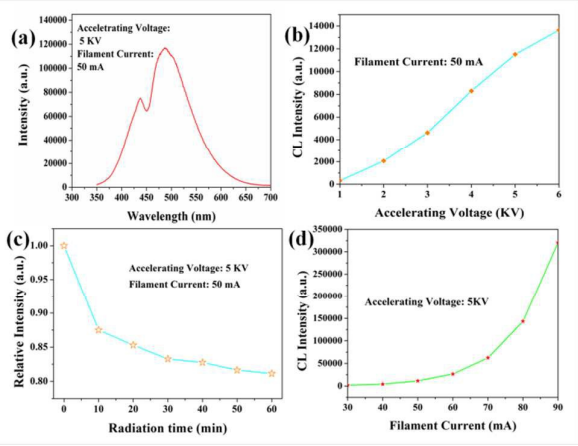

Fig. 6 The cathodoluminescence intensities of the NTSO as a function accelerating voltage (b) and filament current (d). (c) The aging properties of NTSO were measured under V = 5 kV and I = 50 mA.

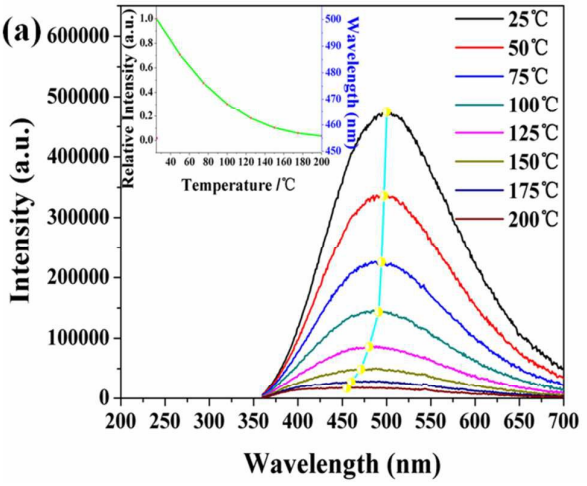

Fig. 7 (a) The temperature dependence of the emission spectra of NTSO, and the inset shows the temperature dependence of the emission intensity and emission peak of NTSO. (b) The configurational coordinate diagram of the ground states and the excited states of Ti^{4+} ions located at two sites.

The degradation property of NTSO has also been investigated to indicate its application in the FEDs. As shown in Fig. 6(c), when the accelerating voltage and filament current are fixed at 5 kV and 50 mA, respectively, at the first 10 min, the CL intensity have an obvious decrease and then shows a nearly parabolic decrease with the continuous electron bombardment. After the radiation for 1h, the intensity of the NTSO falls to 82 % of the initial value, which indicates that the continuous electron radiation has little influence on the NTSO.

The temperature dependence of the PL spectra of the NTSO has also been investigated and exhibited in Fig. 7(a). With the increase of the temperature, the emission intensity of NTSO shows an obvious decrease. At 150 ℃, the integral intensity of NTSO is about 20% of the initial intensity at room temperature. Meanwhile, the blue shift of emission peak changing from 500 nm to 455 nm can be detected with the increase of the temperature. In order to explain this phenomenon, the configurational coordinate diagram of the ground states and the excited states of Ti^{4+} located at two sites has been drew and showed in Fig. 7(b). The electrons absorbing activated energy would be excited to high energy level from the ground state and

then relax to lowest level of the excited energy level, and finally turn back to the ground state along the way ① to emit light. In this process, partial electrons may transfer to TiO_6 site and then return to the ground state along the way ②. With the increase of the temperature, the electron obtaining the thermal activated energy ΔE_1 would show a non-radiative transition to the ground state along the way ③, which is the reason for the temperature quenching. On the other hand, when the partial electrons get the thermal activated energy ΔE_2, they would also transfer to the high energy level of TiO_5, which leads to the blue shift of the emission peak resulted by the increase of the temperature. This phenomenon also proves that the energy transfer between the two sites would happen.

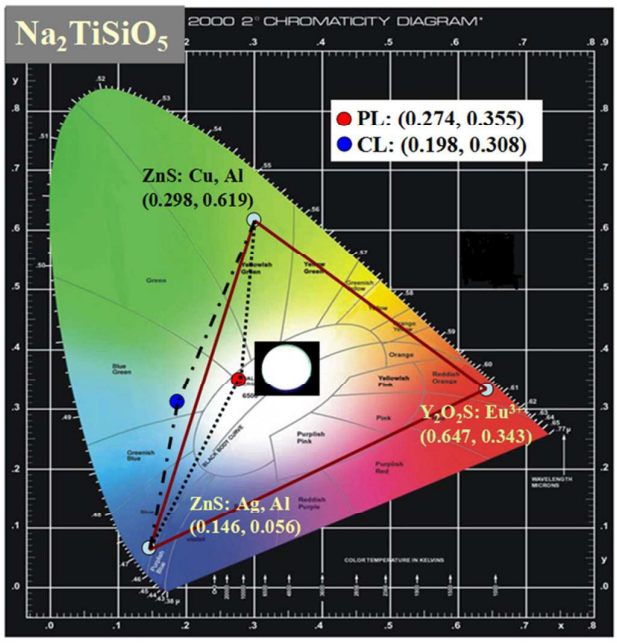

Fig. 8 CIE chromaticity coordinate diagram of NTSO.

The CIE XYZ color space was deliberately designed so that the Y parameter was a measure of the brightness or luminance of a color. The chromaticity of a color was then specified by the two derived parameters x and y, two of the three normalized values which are functions of all three tristimulus values X, Y, and Z. The CIE chromaticity coordinates of NTSO with different excited way have been displayed in Fig. 8. Under the excitation at 260 nm, a white light with chromaticity coordinates of (0.274, 0.355) can be observed, which is in the white region. However, at the low excitation voltage, NTSO emits a cyan light with chromaticity coordinates of (0.198, 0.308), which is out of the triangle area formed by the red light Y_2O_2S: Eu^{3+} with CIE chromaticity coordinate point (0.647, 0.343), the green one ZnS: Cu (0.298, 0.619) and the blue light ZnS: Ag, Al (0.146, 0.056)[33-35]. The results indicates that the cyan light emitting of NTSO can enlarge the color gamut of tricolor FED phosphors and thus increase the display quality of full-color FEDs.

4. Conclusion

In this work, a novel self-activated white-light-emitting phosphor of Na_2TiSiO_5 has been successfully synthesized by high temperature solid-state reaction. The crystal structure of NTSO has been analyzed using the Rietveld refinement, which shows that there are two sites for Ti ions to occupy. Under the excitation at 260 nm, the broad emission band ranging from 400 nm to 650 nm can be observed, which can be well deconvoluted into four well-separated Gaussian components with the peaks at 450 nm, 490 nm, 555 nm and 625 nm, respectively. And the four peaks belong to the emission of TiO_5 (490 nm and 555 nm) and TiO_6 (450 nm and 625 nm), which have been proved by the TRPL spectra and the energy transfer from TiO_5 to TiO_6 would happen. The CL properties of NTSO with a function of the accelerating voltage, filament current and electron radiation time have also been measured. The results indicate that NTSO emits bright cyan light and the intensity of the NTSO still reserves 82 % of the initial value after the radiation for 1h, which indicates that NTSO has potential to be applied in FEDs to enhance the color gamut and improve the display quality.

Acknowledgements

This work was supported by Specialized Research Fund for the Doctoral Program of Higher Education (No. 20120211130003), the National Natural Science Funds of China (Grant No.51372105), State Key Laboratory on Integrated Optoelectronics (No. IOSKL2013KF15) and the Fundamental Research Funds for the Central Universities of Lanzhou University (No. lzujbky-2015-205).

Notes and References:

1 T. Suehiro, N. Hirosaki and R.-J. Xie, ACS Appl. Mater. Interfaces, 2011, 3, 811.
2 S.-K. Kim, J. W. Lee, H.-S. Ee, Y.-T. Moon, S.-H. Kwon, H. Kwon and H.-G. Park, Opt. Express, 2010, 18, 11025.
3 T.-C. Liu, B.-M. Cheng, S.-F. Hu and R.-S. Liu, Chem. Mater., 2011, 23, 3698.
4 Z.-Y. Mao and D.-J. Wang, Inorg. Chem., 2010, 49, 4922.
5 T. Jüstel, H. Nikol and C. Ronda, Angew. Chem., Int. Ed., 1998, 37, 3084.
6 N. Hirosaki, R. Xie, K. Inoue, T. Sekiguchi, B. Dierre and K. Tamura, Appl. Phys. Lett., 2007, 91, 061101.
7 F. A. Kröger, Some Aspects of the Luminescence of Solids; Elsevier: Amsterdam, 1948; pp 159-173.
8 Y. Kotera, T. Sekine, M. Bull. Yonemura, Chem. Soc. Jpn., 1956, 29, 616–619.
9 A. J. H. Macke, J. Solid State Chem., 1976, 18, 337–346.
10 G. Blasse, Philips Res. Rep., 1968, 23, 344–361.
11 T. Yamashita, K. Ueda, J. Solid State Chem., 2007, 180, 1410– 1413.
12 G. Blasse, G. A. M. Dalhoeven, J. Choisnet, F. F. Studer, J. Solid State Chem., 1981, 39, 195–198.
13 L. P. Benderskaya, V. G. Krongauz, M. D. Khalupovskii, J. Appl. Spectrosc., 1974, 20, 238–240.
14 W. L. Konijnendijk, Inorg. Nucl. Chem. Lett., 1981, 17, 129–132.

15 K. Iwasaki, Y. Takahashi, H. Masai, T. Fujiwara, Opt. Express, 2009, 17, 18054–18062.
16 W. L. Konijnendijk, G. Blasse, Mater. Chem. Phys. 1985, 12, 591– 599.
17 G. Blasse, S. J. M. Sas, W. M. A. Smit, W. L. Konijnendijk, Mater. Chem. Phys., 1986, 14, 253–258.
18 T. Kawano, H. Yamane, J. Alloys Compd., 2010, 490, 443–447.
19 S. Abe, H. Yamane, H. Yoshida, Mater. Res. Bull., 2010, 45, 367–372.
20 F.P. Glasser and J. Marr, I Am. &ram. Sot., 62 (1979) 42.
21 I.V. Bussen. E.M. Es'kova, YuP. Men'shikov, A.N. Merkov, A.S. Sakharov, E.I. Semenov and A.P. Khomyakov, Mater. MineraE. Geokhim., (1975) 102 (in Russian),
22 A.V. Nikitin, V.V. Ilyukhin, B.N. Litvin, O.K. Mel'nikov and N.V. Belov, Sov. Phys. Dokl., 1.5 (1964) 625.
23 A. C. Larson and R. B. Von Dreele, "GSAS", General Structure Analysis System, LANSCE, MS-H805, Los Alamos, NewMexico, 1994.
24 P. D. Rack and P. H. Holloway, Mater. Sci. Eng., 1998, 21, 171–219.
25 A.J.H. Macke, J. Solid State Chem., 1976, 18, 337–346.
26 C. H. Huang and T. M. Chen, J. Phys. Chem. C, 2011, 115, 2349.
27 C. H. Huang, T. M. Chen, W. R. Liu, Y. C. Chiu, Y. T. Yeh and S. M. Jang, ACS Appl. Mater. Interfaces, 2010, 2, 259.
28 W. Lv, W. Lü, N. Guo, Y. Jia, Q. Zhao, M. Jiao, B. Shao and H. You, Dalton Trans., 2013, 42, 13071.
29 R. Yu, H. M. Noh, B. K. Moon, B. C. Choi, J. H. Jeong, K. Jang, H. S. Lee and S. S. Yi, Mater. Res. Bull., 2014, 51, 361.
30 Z. Xia, J. Zhuang and L. Liao, Inorg. Chem., 2012, 51, 7202
31 Z. Xia, J. Zhuang, A. Meijerink and X. Jing, Dalton Trans., 2013, 42, 6327.
32 C. Feldman, Phys. Rev., 1960, 117, 455.
33 F. L. Zhang, S. Yang, C. Stoffers, J. Penczek, P. N. Yocom, D. Zaremba, B. K. Wagner and C. J. Summers, Appl. Phys. Lett., 1998, 72, 2226.
34 M. Kottaisamy, K. Horikawa, H. Kominami, T. Aoki, N. Azuma, T. Nakamura, Y. Nakanishi and Y. Hatanaka, J. Electrochem. Soc., 2000, 147, 1612.
35 M. K. Patra, K. Manzoor, M. Manoth, S. R. Vadera and N. Kumar, J. Lumin., 2008, 128, 267.

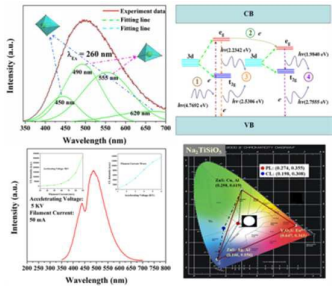

Self-activated light emitting phosphor of Na_2TiSiO_5 can emit a white light and cyan light under the different excitation ways.